Nonlocality-Induced Front-Interaction Enhancement

L. Gelens,[1,2] D. Gomila,[2] G. Van der Sande,[1] M. A. Matías,[2] and P. Colet[2]

[1]*Department of Applied Physics and Photonics, Vrije Universiteit Brussel, Pleinlaan 2, 1050 Brussels, Belgium*
[2]*IFISC, Instituto de Física Interdisciplinar y Sistemas Complejos (CSIC-UIB), Campus Universitat Illes Balears, E-07122 Palma de Mallorca, Spain*

(Received 14 December 2009; published 15 April 2010)

We demonstrate that nonlocal coupling strongly influences the dynamics of fronts connecting two equivalent states. In two prototype models we observe a large amplification in the interaction strength between two opposite fronts increasing front velocities several orders of magnitude. By analyzing the spatial dynamics we prove that way beyond quantitative effects, nonlocal terms can also change the overall qualitative picture by inducing oscillations in the front profile. This leads to a mechanism for the formation of localized structures not present for local interactions. Finally, nonlocal coupling can induce a steep broadening of localized structures, eventually annihilating them.

DOI: 10.1103/PhysRevLett.104.154101 PACS numbers: 05.45.Yv, 05.65.+b, 42.65.Tg, 89.75.−k

Most studies on the emergence of complex behavior in spatially extended systems consider that spatial coupling is either local or alternatively global (all to all coupling) [1,2]. More recently, systems with nonlocal (or intermediate- to long-range) coupling have received increasing attention, as nonlocal interactions are known to be relevant in diverse fields, ranging from Josephson junction arrays [3] and chemical reactions [4,5], to several problems in biology and ecology [6], such as the neural networks underlying mollusk patterns [7,8], ocular dominance stripes and hallucination patterns [9], and population dynamics [10]. A nonlocal interaction may emerge from a physical or chemical mechanism that couples points far apart in space, e.g., a long-range interaction [11], or from the adiabatic elimination of a slow variable [12,13]. Novel phenomena emerging genuinely from nonlocality, such as power-law correlations [12,14], multiaffine turbulence [4], and chimera states [15,16] have been reported. Moreover, recent works have reported the effects of nonlocality on the dynamics of fronts, patterns and localized structures (LS), for instance the tilting of snaking bifurcation lines [17] and changes in the size of LS [18], the effects of two-point nonlocality on convective instabilities [19], the nonlocal stabilization of vortex beams [20], or changes in the interaction between solitons [21], and in the velocity of propagating fronts [22].

The main goal of this Letter is to show the crucial relevance of nonlocality on the interaction of fronts connecting two equivalent states in one dimensional systems, as well as on the formation of LS arising from the interaction of two such fronts [23]. Interaction between two monotonic fronts is always attractive, so any domain of one state embedded in the other shrinks and disappears. However, fronts with oscillatory tails can lock at specific distances leading to stable LS. Here we show that oscillatory tails, and therefore stable LS can appear as an effect of repulsive nonlocal interactions. Repulsive (inhibitory) interactions are common, for instance, in neural field theories [8,9] and genetic networks [24]. Our result is generic and can be qualitatively understood from the interplay between nonlocality, which couples both sides of the front, and repulsiveness which induces a small depression at the lower side and a small hill at the upper part. Altogether this leads to oscillatory tails as qualitatively obtained from the spatial dynamics.

A prototypical model of a spatially extended system with two equivalent steady states is the real Ginzburg-Landau equation (GLE) [2,25]. We consider the 1D *nonlocal* real GLE

$$\frac{\partial E(x)}{\partial t} = (\mu - s)E(x) + \frac{\partial^2 E(x)}{\partial x^2} - E^3(x) + sF(x), \quad (1)$$

being $E(x)$ a real field and μ the gain parameter. The diffusion and the nonlinear term have been scaled to one without loss of generality. Equation (1) has both a local (diffusive) and a (linear) nonlocal spatial coupling

$$F(x) = \int_{-\infty}^{\infty} \theta_\sigma(x - x')E(x')dx', \quad (2)$$

where θ_σ is the spatial nonlocal interaction function (or kernel) and σ indicates the spatial extension of the coupling. For the sake of simplicity, we consider here a Gaussian kernel, $\theta_\sigma(x - x') = (1/\sqrt{2\pi}\sigma)e^{-(x-x')^2/(2\sigma^2)}$, although the results presented in this work do not depend qualitatively on its precise shape, provided it is positively defined. Gaussian kernels appear in contexts such as mollusk pigmentation patterns [26] and Neuroscience [9,27]. The nonlocal function $F(x)$ includes also a local contribution. This contribution is compensated for by the term $-sE(x)$, such that in the limit $\sigma \to 0$ one recovers the same results as for the local GLE.

The profile of GLE fronts is known analytically [28], and the interaction with an opposite front located at a distance d much larger than the front width can be calcu-

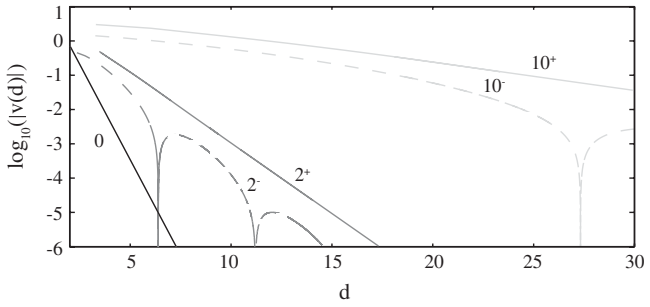

FIG. 1. Front velocity as a function of d. $\mu = 3$, $|s| = 1$, and σ is taken to be 0, 2 and 10, depicted in the figure as $\sigma^{\mathrm{sgn}(s)}$.

lated perturbatively, yielding the following result for the relative velocity $v(d)$ [28],

$$v(d) = \dot{d} = ce^{-\gamma d}, \tag{3}$$

with $c = -24\sqrt{2\mu}$ and $\gamma = \sqrt{2\mu}$. The nonlocal effects in front dynamics can be quantified by looking at the deviations from the interaction given by Eq. (3), stemming solely from a local interaction coupling. Therefore we have studied the front velocity $v(d)$ for different kernel widths σ keeping all other parameters fixed and taking the system size much larger than σ. The results are plotted in Fig. 1. The *local* case, Eq. (3), is the straight line labeled with 0 (as $\sigma = 0$). In the nonlocal case ($\sigma \neq 0$), a large qualitative difference in behavior is observed depending on the sign of s.

As shown in Fig. 1, for an attractive (activatory) interaction ($s > 0$), the logarithm of the velocity decreases linearly with the distance, such that the exponential dependence of the velocity with the distance given by Eq. (3) still holds with an effective γ whose value is strongly reduced by the nonlocality. As a consequence the range of spatial interaction, $1/\gamma$, increases with the kernel width σ. Even for moderate values of σ, fronts move several orders of magnitude faster than for the local GLE. Figure 2 shows the change of the value of the effective exponent γ as a function of σ. Moreover, the inset shows that γ, to a very good extent, follows a linear dependence with the inverse of the kernel width σ, provided that σ is at least as large as the front width. Therefore, we can conclude that rescaling γ to γ/σ the effective interaction between two fronts follows a universal exponential law (except for a small dependence on the strength of interaction s). It is interesting to notice, however, that the width of the front, defined by the half width at half the maximum (HWHM) does not show this scaling with $1/\sigma$ cf. Fig. 3(a). This can be understood by noticing that while the general shape of the front is mainly dominated by the local, diffusive, coupling, in turn the nonlocal coupling modifies substantially the exponential tails, which are responsible of the long-range interaction that influences the front velocity.

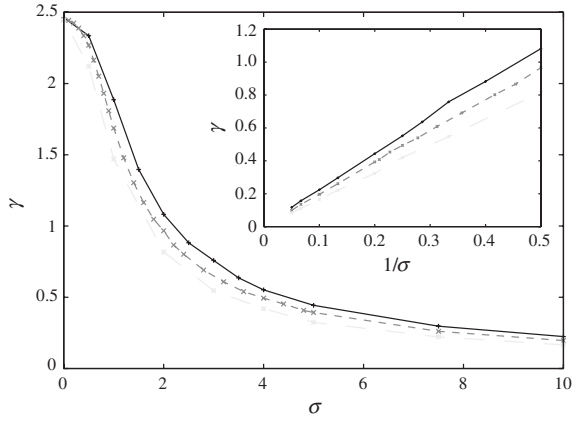

FIG. 2. γ as a function of σ. Inset: γ as a function of $1/\sigma$. The black solid, dark gray dashed, and light gray dashed curves have $\mu = 3$, and $s = 0.5$, 1, and 2, respectively.

For $s < 0$, i.e., for a repulsive (inhibitory) interaction, the exponential law, Eq. (3), no longer holds. Nevertheless, the magnitude of the envelope of the front velocity is still dominated qualitatively by (3), as shown in Fig. 1. In this case, the velocity becomes zero at regular intervals of the distance d between two fronts. At these positions the fronts are locked leading to the formation of LS. These LS, not present in the GLE, come into existence by the creation of oscillatory tails when a nonlocal term with $s < 0$ is added.

A quantitative characterization is obtained from the *spatial dynamics* of Eq. (1). Considering a spatial perturbation to the homogeneous solution of the form $E = \sqrt{\mu} + \epsilon \exp(\lambda x)$, one finds

$$-2\mu - s + \lambda^2 + se^{\lambda^2\sigma^2/2} = 0. \tag{4}$$

Eigenvalues come in pairs $\pm\lambda$. The shape of the front is determined by the eigenvalue λ_1 with real part closest to zero, as in the spatial dynamics all the other directions are damped faster when approaching the fixed point (homogeneous solution). By determining where λ_1 goes from being purely real to complex, one can find the boundary A separating fronts having monotonic and oscillatory tails. As shown in Fig. 3(b), for kernel widths σ at least as large as the front width, the front profile always shows oscillatory tails for $s < 0$ and as a consequence LS can arise as displayed in Fig. 4. For smaller kernel widths an increasingly large nonlocal strength is needed for LS to be formed

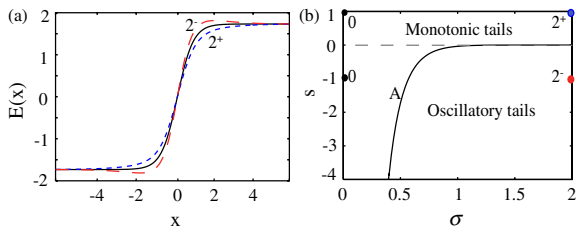

FIG. 3 (color online). Nonlocal GLE, Eq. (1) with $\mu = 3$: (a) Front profiles for $s = 0$ (black line) and $s = \pm 1$ with $\sigma = 2$, labeled in the figure as $\sigma^{\mathrm{sgn}(s)}$. (b) The curve A is the boundary in the (σ, s) space between the presence of oscillatory or monotonic tails of a front.

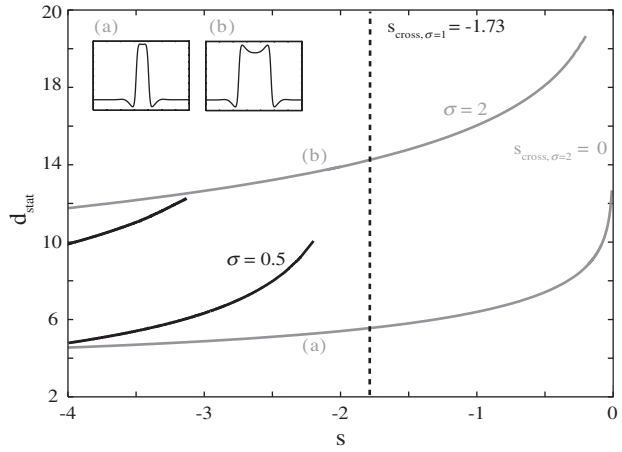

FIG. 4. Stationary widths of stable LS for the nonlocal GLE ($\mu = 3$). Black (gray) line corresponds to $\sigma = 0.5$ ($\sigma = 2$). Insets show examples of LS profiles for $\sigma = 2$. $s_{\mathrm{cross},\sigma}$, given by line A in Fig. 3, indicates the point where the spatial eigenvalues go from being complex conjugate to purely real.

(see line A in Fig. 3). To describe the interaction of fronts with oscillatory tails Eq. (3) must be modified. An appropriate ansatz is the following:

$$v = \dot{d} = c\cos[\zeta(s,\sigma)d]e^{-\gamma(s,\sigma)d}, \tag{5}$$

where $\zeta(s,\sigma)$ is determined by the complex part of the most underdamped spatial eigenvalue of Eq. (4), such that $\zeta = 0$ in the region of monotonic tails. Equation (5) adequately describes the dependence of the velocity with the distance indicated in Fig. 1.

In summary, for the real GLE one finds an enhancement of the interaction due to nonlocality, that leads to the appearance of oscillatory tails and LS for a repulsive interaction and increase of the front velocity if the interaction is attractive.

We check the generality of these findings for the parametrically forced complex Ginzburg-Landau equation (PCGLE) whose fronts show oscillatory tails already in the local case and form LS [29,30]. The PCGLE is the generic amplitude equation for oscillatory systems parametrically forced at twice the natural frequency [31]. The nonlocal version of the PCGLE can be written as

$$\frac{\partial E(x)}{\partial t} = (1+i\alpha)\frac{\partial^2 E(x)}{\partial x^2} + [(\mu+i\nu) - se^{i\phi_s}]E(x) - (1+i\beta)|E(x)|^2E(x) + pE^*(x) + se^{i\phi_s}F(x), \tag{6}$$

where μ measures the distance from the oscillatory instability threshold, ν is the detuning between the driving and the natural frequencies, $p > 0$ is the forcing amplitude, α and β represent the linear and nonlinear dispersion. The term $se^{i\phi_s}F(x)$ describes the nonlocal response of the material taking the same form as in the study of the GLE (2). Here we consider $s > 0$ with $\phi_s = 0$ and $\phi_s = \pi$ in correspondence with attractive and repulsive interactions discussed previously. Again, the linear contribution has been compensated in the term $-se^{i\phi_s}E(x)$.

Figure 5 shows the width of the stable LS locked at the first and second oscillations as a function of the nonlocal strength s. The insets show the LS spatial profile. Whereas in the real GLE, LS existed only for $s < 0$ (see Fig. 4), in the PCGLE, LS also exist for a finite range of positive values of $s\cos(\phi_s)$ ($\phi_s = 0$). This is shown in Fig. 5 for $\sigma = 2$ where the bifurcation branch abruptly ends around $s_{\mathrm{cross}} = 0.556$. This can be explained again by studying the spatial eigenvalues of the system. In this case there are two pairs of complex conjugate eigenvalues with small real part λ_l and λ_{nl} which play a relevant role. Figure 6(a) shows the dependence of the real and imaginary parts of these two eigenvalues for $\sigma = 1.3$ and 2 as a function of s. For small s the spatial dynamics is dominated by λ_l, the eigenvalue already present in the local case. Increasing s, the real part of this eigenvalue becomes slightly larger while the real part of λ_{nl} clearly decreases. For $\sigma = 2$, the real part of the two eigenvalues crosses at $s_{\mathrm{cross}} = 0.556$. Beyond that value the spatial dynamics is governed by λ_{nl} whose corresponding spatial length scale $[\mathrm{Im}(\lambda_{nl})]$ is an order of magnitude larger than the one corresponding to λ_l. As a result, the branch of LS experiences dramatic sharpening in Fig. 5, as the LS broaden with an order of magnitude. Figure 6(b) shows the locus of the crossing point in the (σ, s) plane for $\phi_s = 0$. For large values of σ, the crossing point moves towards $s = 0$, while for $\sigma < 1.43$ the crossing never takes place and the spatial dynamics is always dominated by λ_l.

For $\phi_s = \pi$, nonlocality only modifies slightly the preexisting oscillatory tails of the PCGLE. The branches of LS end for negative values of $s\cos(\phi_s)$ close to the modulational instability point of the background states (that for $\sigma = 2$ is at $s\cos(\phi_s) \sim -3$). This MI point, that was originated by the nonlocality in the GLE, is already present in the local form of the PCGLE but is enhanced by the nonlocal interactions.

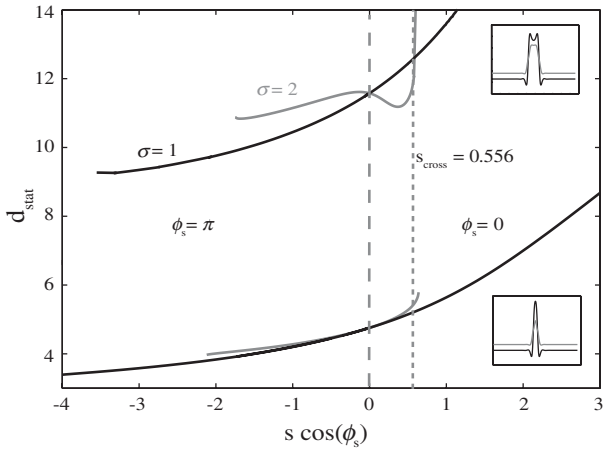

FIG. 5. Stationary widths of stable LS for $\alpha = 1$, $\beta = 0$, $\mu = 0$, $\nu = 2$ and $p = 2.7$. $\sigma = 1$ (black line) and 2 (gray line). Insets show the transverse profile of the LS.

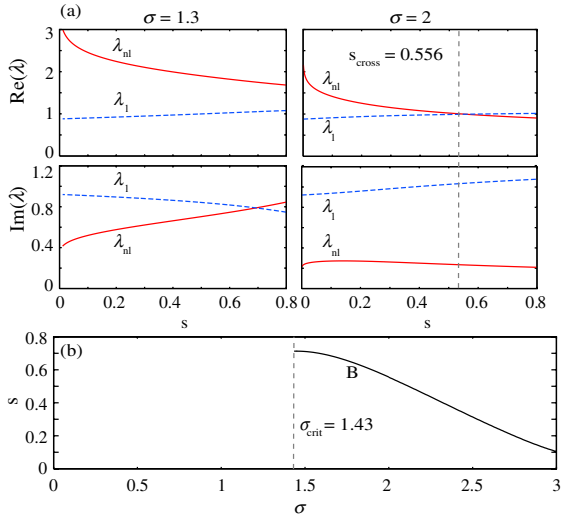

FIG. 6 (color online). (a) Dependence of the absolute value of the real and imaginary parts of the two dominant complex quartets of spatial eigenvalues in the nonlocal PCGLE for $\sigma = 1.3$ and $\sigma = 2$ as a function of s. Other parameters as in Fig. 5. (b) The curve B depicts the locus in the (σ, s) plane of the points where the absolute values of the real parts of λ_l and λ_{nl} cross.

In conclusion, we have demonstrated the large impact of a linear nonlocal term on the interaction of fronts connecting two equivalent states. The most striking result is the possibility of obtaining a novel class of self-organized stable localized structures in systems exhibiting fronts with no tails, like the real GLE. This is achieved through a nonlocal repulsive interaction that modifies the profile of the fronts introducing or damping out oscillations. In addition, we have observed an order of magnitude increase of the front velocity due to an enhancement of the interaction between two fronts. Finally, we have shown that nonlocal interactions can also smooth out the front oscillations greatly increasing their wavelength such that the LS become much wider and eventually disappear.

The characterization of the effects of nonlocal coupling on the front properties and dynamics can allow the identification, from both theoretical and experimental data, of different sources of nonlocality. For instance, domain walls have long been studied in photorefractive media [32], which have a large nonlocal response, but its effects on the front dynamics have never been identified. Nonlocal interactions are also common in biology, chemistry, and other fields, and they can have a constructive role by enhancing the propagation of information between distant parts of the system.

This work was supported by the Belgian Science Policy Office under grant No. IAP-VI10, and by the Spanish Ministry of Science and Innovation and FEDER under grant FIS2007-60327. G. VdS. and L. G. acknowledge support by the Research Foundation—Flanders (FWO). We thank Professor E. Knobloch for interesting discussions.

[1] Y. Kuramoto, *Chemical Oscillations, Waves and Turbulence* Springer Series in Synergetics (Springer, Berlin, 1984), 3rd ed.
[2] M. Cross and P. Hohenberg, Rev. Mod. Phys. **65**, 851 (1993).
[3] J. R. Philips *et al.*, Phys. Rev. B **47**, 5219 (1993).
[4] Y. Kuramoto, D. Battogtokh, and H. Nakao, Phys. Rev. Lett. **81**, 3543 (1998).
[5] S.-I. Shima and Y. Kuramoto, Phys. Rev. E **69**, 036213 (2004).
[6] J. Murray, *Mathematical Biology* (Springer, New York, 2002), 3rd ed.
[7] B. Ermentrout, J. Campbell, and G. Oster, Veliger **28**, 369 (1986).
[8] S. Coombes, Biol. Cybern. **93**, 91 (2005).
[9] B. Ermentrout, Rep. Prog. Phys. **61**, 353 (1998).
[10] E. Hernández-García and C. López, Phys. Rev. E **70**, 016216 (2004).
[11] P. Pedri and L. Santos, Phys. Rev. Lett. **95**, 200404 (2005).
[12] Y. Kuramoto, Prog. Theor. Phys. **94**, 321 (1995).
[13] D. Tanaka and Y. Kuramoto, Phys. Rev. E **68**, 026219 (2003).
[14] Y. Kuramoto and H. Nakao, Phys. Rev. Lett. **76**, 4352 (1996).
[15] D. Abrams and S. Strogatz, Phys. Rev. Lett. **93**, 174102 (2004).
[16] G. Sethia, A. Sen, and F. M. Atay, Phys. Rev. Lett. **100**, 144102 (2008).
[17] W. J. Firth, L. Columbo, and A. Scroggie, Phys. Rev. Lett. **99**, 104503 (2007).
[18] L. Gelens *et al.*, Phys. Rev. A **75**, 063812 (2007); L. Gelens *et al.*, Phys. Rev. A **77**, 033841 (2008).
[19] R. Zambrini and F. Papoff, Phys. Rev. Lett. **94**, 243903 (2005).
[20] S. Skupin, M. Saffman, and W. Krolikowski, Phys. Rev. Lett. **98**, 263902 (2007).
[21] A. Dreischuh *et al.*, Phys. Rev. Lett. **96**, 043901 (2006).
[22] Y. Maruvka and M. Shnerb, Phys. Rev. E **75**, 042901 (2007).
[23] M. Pesch *et al.*, Phys. Rev. Lett. **99**, 153902 (2007).
[24] U. Alon, *An Introduction to Systems Biology of Biological Circuits* (Chapman & Hall/CRC, Boca Raton, FL, 2007).
[25] I. Aranson and L. Kramer, Rev. Mod. Phys. **74**, 99 (2002).
[26] A. Boettiger, B. Ermentrout, and G. Oster, Proc. Natl. Acad. Sci. U.S.A. **106**, 6837 (2009).
[27] B. Hellwig, Biol. Cybern. **82**, 111 (2000).
[28] P. Coullet, C. Elphick, and D. Repaux, Phys. Rev. Lett. **58**, 431 (1987).
[29] D. Gomila *et al.*, Phys. Rev. Lett. **87**, 194101 (2001).
[30] A. Yochelis, J. Burke, and E. Knobloch, Phys. Rev. Lett. **97**, 254501 (2006).
[31] P. Coullet *et al.*, Phys. Rev. Lett. **65**, 1352 (1990).
[32] V. B. Taranenko, K. Staliunas, and C. O. Weiss, Phys. Rev. Lett. **81**, 2236 (1998); A. Esteban-Martin *et al.*, Appl. Phys. B **85**, 117 (2006).